

Microphase Separation in Polyelectrolytic Diblock Copolymer Melt : Weak Segregation Limit

Rajeev Kumar and M.Muthukumar *

Dept. of Polymer Science & Engineering,

Materials Research Science & Engineering Center,

University of Massachusetts, Amherst, MA-01003, USA.

ABSTRACT

We present a generalized theory of microphase separation for charged-neutral diblock copolymer melt. Stability limit of the disordered phase for salt-free melt has been calculated using Random Phase Approximation (RPA) and self-consistent field theory (SCFT). Explicit analytical free energy expressions for different classical ordered microstructures (lamellar, cylinder and sphere) are presented. We demonstrate that chemical mismatch required for the onset of microphase separation (χ^*N) in charged-neutral diblock melt is higher and the period of ordered microstructures is lower than those for the corresponding neutral-neutral diblock system. Theoretical predictions on the period of ordered structures in terms of Coulomb electrostatic interaction strength, chain length, block length, and the chemical mismatch between blocks are presented. SCFT has been used to go beyond the stability limit, where electrostatic potential and charge distribution are calculated self-consistently. Stability limits calculated using RPA are in perfect agreement with the corresponding SCFT calculations. Limiting laws for stability limit and the period of ordered structures are presented and comparisons are made with an earlier theory. Also, transition boundaries between different morphologies have been investigated.

* To whom any correspondence should be addressed, Email : muthu@polysci.umass.edu

I. INTRODUCTION

Science behind the complex behavior of amphiphilic systems continues to be of interest to scientific community. A great deal of theoretical^{1,2,3,4,5,6,7,8} and experimental efforts^{9,10,11,12,13,14} have been made to study this behavior. Especially, self-assembly of amphiphiles¹¹ is of significant importance in understanding many biological systems. An amphiphilic diblock copolymer system has applications such as encapsulation^{12,13} and drug delivery¹⁴, which are dependent on self-assembly of macromolecules.

Self-assembly of neutral block copolymers in concentrated regimes, has already been studied extensively in the last three decades. Seminal work in developing theory for microdomains in diblock copolymer melt was done by Helfand¹⁵ *et al*, where unit cell approximation was used to calculate the properties for sharp interfaces (strong segregation limit (SSL)). Later on, Leibler¹⁶ calculated morphology diagrams in weak segregation limit (WSL) using the random phase approximation (RPA), when the system is on the verge of transformation from disordered to ordered phases and interfaces between the ordered domains are diffuse. Few years later, Semenov¹⁸ and Ohta¹⁹ *et al* calculated morphology diagrams in SSL taking into account a sharp interface between the domains. Semenov used ground state dominance and Ohta *et al* extended the RPA method developed by Leibler to SSL. Afterwards, Muthukumar^{31,32} *et al* and Matsen³⁷ *et al* bridged the gap between WSL and SSL theories by using density functional theory (DFT) and SCFT respectively. To go beyond mean field, fluctuations of order parameter were included by Fredrickson²⁹ *et al*, Olvera de la cruz³⁰ and Muthukumar³³.

Although we have a sound understanding of neutral copolymers, our understanding of charged copolymers is inadequate. A number of researchers have tried to explore charged diblock systems. Some of these efforts are invested in studying dilute solutions (micelle regime)^{20,23} and others have been carried out in the concentrated regime^{3,4,5,24,25}. The fundamental question is how Coulomb interactions affect the relative stabilities of ordered morphologies. First work in this direction was carried out by Marko and Rabin³ who explored charged copolymers in both the melts and solutions. In their study, they presented the effect of degree of ionization and salt on critical parameters for weak segregation in melt and studied micelle behaviour also. But they did not consider any ordered microstructures for melts. Recently, SCFT for polyelectrolytic systems has been developed by Shi³⁵ *et al*

and Wang³⁶ *et al* .

In this paper, we have considered microphase separation in diblock copolymer melts, formed out of polyelectrolyte (A) block and neutral (B) block. RPA is presented in Sec. II A and SCFT equations are briefly presented in Sec. II B. Calculated results and conclusions are presented in Sec. III and IV, respectively.

II. THEORY

We consider a system of n block copolymer chains, each containing a total of N segments of two species (A and B) with f as the fraction of the block A . Number of segments in blocks A and B is represented by N_A and N_B , respectively, so that ($f = N_A/N, N = N_A + N_B$). Block A is taken to be polyelectrolytic (negatively charged) and we assume that there are n_c counterions released by the charged block. In addition to this, there are n_γ ions of species γ coming from the added salt (in total volume Ω) so that the whole system is globally electroneutral. Let Z_i be the valency of the i^{th} charged species. Subscripts $A, B, c, +$ and $-$ are used to represent monomer A, B , counterion from block A , positive and negative salt ions, respectively. The degree of ionization of the A block per chain is taken to be α so that each of the $f\alpha N$ segments of A block chain carry a charge of eZ_A , where e is the electronic charge. So, there are $N(1 - f\alpha)$ uncharged segments in a chain. Recently, it has been shown that specific charge distributions along the backbone play a significant role in the physics of polyelectrolytes³⁶. In our current study, we consider smeared charge distribution i.e. *each* segment of block A has charge $e\alpha Z_A$. We represent copolymer chain as a continuous curve of length Nl , where l is the Kuhn segment length. For the treatment shown below, we assume that volume occupied by each A and B monomer is the same ($= l^3 \equiv 1/\rho_o, \rho_o$ being the bulk density) and that the system is incompressible so that $\Omega = nNl^3$. We use an arc length variable s_j to represent any segment along the backbone of j^{th} chain. In this notation, A block in j^{th} chain is represented by s_j ($0 \leq s_j \leq N_A l$). Also, the position vector for a particular segment is represented by $R_j(s_j)$. For this system, Helmholtz free energy F can be written within Edward's formalism by:

$$\exp\left(-\frac{F}{k_B T}\right) = \frac{1}{n! n_c! \prod_\gamma n_\gamma!} \int \prod_{j=1}^n D[R_j] \int \prod_{i=1}^{n_c + \sum_\gamma n_\gamma} dr_i \exp\left\{-\frac{3}{2l} \sum_{j=1}^n \int_0^{Nl} ds_j \left(\frac{\partial R_j}{\partial s_j}\right)^2\right\}$$

$$\begin{aligned}
& -\frac{1}{2l^2} \sum_{j=1}^n \sum_{k=1}^n \left[\int_0^{N_{Al}} ds_j \int_0^{N_{Al}} ds_k V_{AA}[R_j(s_j) - R_k(s_k)] \right. \\
& + \int_{N_{Al}}^{Nl} ds_j \int_{N_{Al}}^{Nl} ds_k V_{BB}[R_j(s_j) - R_k(s_k)] \\
& \left. + 2 \int_0^{N_{Al}} ds_j \int_{N_{Al}}^{Nl} ds_k V_{AB}[R_j(s_j) - R_k(s_k)] \right] \\
& - \frac{1}{l} \sum_{j=1}^n \sum_{m=1}^{n_c + \sum_{\gamma} n_{\gamma}} \left[\int_0^{N_{Al}} ds_j V_{Am}[R_j(s_j) - r_m] + \int_{N_{Al}}^{Nl} ds_j V_{Bm}[R_j(s_j) - r_m] \right] \\
& - \frac{1}{2} \sum_{m=1}^{n_c + \sum_{\gamma} n_{\gamma}} \sum_{p=1}^{n_c + \sum_{\gamma} n_{\gamma}} V_{mp}[r_m - r_p] \left. \right\} \prod_r \delta[\hat{\rho}_A(r) + \hat{\rho}_B(r) - \rho_0] \quad (1)
\end{aligned}$$

Here, $k_B T$ is Boltzmann constant times the absolute temperature. $V_{AA}(r)$, $V_{BB}(r)$ and $V_{AB}(r)$ are the interaction energies between segments of different types separated by distance $\mathbf{r} = |r|$ so that

$$V_{AA}(r) = w_{AA} \delta(\mathbf{r}) + \frac{Z_A^2 e^2 \alpha^2}{\epsilon k_B T} \frac{1}{r} \quad (2)$$

$$V_{BB}(r) = w_{BB} \delta(\mathbf{r}) \quad (3)$$

$$V_{AB}(r) = w_{AB} \delta(\mathbf{r}) \quad (4)$$

where w_{AA} , w_{BB} and w_{AB} are the intersegment excluded volumes arising from the short range interactions, $\delta(\mathbf{r})$ is Dirac delta function and ϵ is *position independent effective* dielectric constant of the medium (in units of $4\pi\epsilon_0$ where ϵ_0 is the permittivity of vacuum). In writing $V_{AA}(r)$, it is assumed that total charge of any chain is uniformly distributed along A block (smeared charge distribution). Interactions between polymer segments and small charged molecules (counterions and coions) are accounted for by treating small ions as point charges so that they have zero excluded volume and are purely electrostatic in nature. These interactions, represented by $V_{Am}(r)$, $V_{Bm}(r)$ and $V_{mp}(r)$ in Eq. (1), are given by

$$V_{Am}(r) = \frac{Z_A Z_m e^2 \alpha}{\epsilon k_B T} \frac{1}{r} \quad (5)$$

$$V_{Bm}(r) = 0 \quad (6)$$

$$V_{mp}(r) = \frac{Z_m Z_p e^2}{\epsilon k_B T} \frac{1}{r} \quad (7)$$

The Dirac delta function involving $\hat{\rho}_A(r)$ and $\hat{\rho}_B(r)$ enforce the incompressibility of the system at all locations, where $\hat{\rho}_A(r)$ and $\hat{\rho}_B(r)$ are *microscopic* monomer number densities

defined as

$$\hat{\rho}_A(r) = \frac{1}{l} \sum_{j=1}^n \int_0^{N_A l} ds_j \delta(r - R_j(s_j)) \quad (8)$$

$$\hat{\rho}_B(r) = \frac{1}{l} \sum_{j=1}^n \int_{N_A l}^{N l} ds_j \delta(r - R_j(s_j)) \quad (9)$$

A. WSL - Random Phase Approximation

1. Stability Limit

Near the stability limit of the melt, densities of all components in the inhomogeneous phase deviate slightly from their average values in the homogeneous phase. So, the free energy of the inhomogeneous phase can be obtained by expanding the corresponding free energy expression for the homogeneous phase about the average densities. Neglecting cubic and higher order terms in densities, the free energy of the inhomogeneous phase is obtained in terms of the order parameter $\phi(r)$ (see Appendix A) and has the form:

$$F = F_0 + \delta F(\phi) + O(\phi^3), \quad (10)$$

where the order parameter ϕ is the same as that used for neutral block copolymer melts, given by

$$\phi(r) = \langle \delta \hat{\rho}_A(r) \rangle = \langle \hat{\rho}_A(r) \rangle - f \rho_0. \quad (11)$$

F_0 is the free energy of the homogeneous phase and is given by a Flory-type equation:

$$\frac{F_0}{k_B T} = \sum_{i=c,+,-} n_i \ln(n_i) - \frac{\kappa^3}{12\pi} + \chi_{AB} f(1-f) \quad (12)$$

In writing F_0 , linear and constant terms have been ignored. In Eq. (12), χ_{AB} and $\kappa^{-1} = r_D$ are Flory's chi parameter and the Debye screening length, respectively. r_D is given by

$$\kappa^2 = 4\pi l_B \left(\frac{n_c}{\Omega} Z_c^2 + \sum_{\gamma=+,-} \frac{n_\gamma}{\Omega} Z_\gamma^2 \right) \quad (13)$$

and $l_B = e^2/\epsilon k_B T$ stands for the Bjerrum length (in units of $4\pi\epsilon_0$). In Eq. (12), the first term corresponds to the translational entropy of small ions, κ^3 term accounts for counterions and coions correlation effect and χ_{AB} term gives the contribution of chemical mismatch between blocks.

The second degree term in ϕ defines the structure factor ($S(k)$) and is given by:

$$\delta F(\phi) = \frac{1}{2} \int \frac{d^3k}{(2\pi)^3} S^{-1}(k) \phi(k) \phi(-k) \quad (14)$$

$$S^{-1}(k) = S_0^{-1}(k) + S_1^{-1}(k) \quad (15)$$

$$S_0^{-1}(k) = Q(x) - 2\chi_{AB}l^3 \quad (16)$$

$$Q(x) = \frac{g(1, x)}{\rho_0 N \{g(f, x)g(1-f, x) - [g(1, x) - g(f, x) - g(1-f, x)]^2/4\}} \quad (17)$$

$$S_1^{-1}(k) = \frac{4\pi l_B Z_A^2 \alpha^2 N l^2}{6x + \kappa^2 N l^2} \quad (18)$$

In Eq. (15), $S_0^{-1}(k)$ is the contribution due to short range excluded volume interactions and $S_1^{-1}(k)$ is due to the long range Coulomb interactions present in the system. $g(f, x)$ is the Debye function given by

$$g(f, x) = \frac{2(fx + e^{-fx} - 1)}{x^2}, \quad x = \frac{k^2 N l^2}{6} = k^2 R_g^2 \quad (19)$$

Note that Eqs. (14 - 18) are the same as in Ref.³.

2. Limiting Laws

To understand the qualitative behaviour of the system at the stability limit, a scaling analysis is presented here for two limiting cases. In order to carry out the scaling analysis, the complicated equation for $S_0^{-1}(k)$ is approximated by an expression, used previously for neutral block copolymers¹⁹, which reproduces $S_0^{-1}(k)$ with about 5 % accuracy. Using the approximate expression, Eq. (14) becomes:

$$\delta F\{\phi\} = \frac{1}{2\rho_0 N} \int \frac{d^3k}{(2\pi)^3} \left\{ B(f)k^2 + \frac{A(f)}{k^2} + \frac{C(l_B)}{k^2 + \kappa^2} - \bar{\chi} \right\} \phi(k) \phi(-k) \quad (20)$$

$$B(f) = \frac{Nl^2}{12f(1-f)} \quad (21)$$

$$A(f) = \frac{9}{Nl^2 f^2 (1-f)^2} \quad (22)$$

$$C(l_B) = 4\pi l_B Z_A^2 \alpha^2 \rho_0 N \quad (23)$$

$$\bar{\chi} = 2\chi_{AB} N \rho_0 l^3 - \frac{s(f)}{2f^2(1-f)^2} \quad (24)$$

Here, $s(f)$ is a parameter used to reproduce $S_0^{-1}(k)$. At the stability limit, $S(k)$ diverges at the wave-vector $k = k^*$ and the second degree term δF in free energy vanishes at $k = k^*$ and $\chi_{AB}N = \chi_{AB}^*N$. In the case of neutral block copolymers (i.e. $C(l_B) = 0$), the

divergence corresponds to $k^* = (A/B)^{1/4} \sim N^{-1/2}$ so that the period $D = 2\pi/k^* \sim N^{1/2}$. Hence, δF vanishes at $\bar{\chi}^* = 2\sqrt{AB}$ so that $\chi_{AB}^* N$ is given by expression

$$(\chi_{AB}^* N)_{neutral} = \frac{1}{\rho_0 l^3} \left[\frac{s(f)}{4f^2(1-f)^2} + \sqrt{\frac{3}{4f^3(1-f)^3}} \right] \quad (25)$$

Now, for charged block copolymers, consider the two limiting cases: (i) $k^2 \ll \kappa^2$ and (ii) $k^2 \gg \kappa^2$. In terms of the Debye screening length, these cases correspond to $r_D \ll D$ and $r_D \gg D$, respectively.

Case (i): $r_D \ll D$

In this regime, the structure factor becomes

$$S^{-1}(k) \simeq Bk^2 + \frac{A}{k^2} - \left(\bar{\chi} - \frac{C}{\kappa^2} \right) \quad (26)$$

The maxima of the structure factor corresponds to $k^* = (A/B)^{1/4} \sim N^{-1/2}$ so that the period $D = 2\pi/k^* \sim N^{1/2}$ and is *independent* of degree of ionization of charged block. So, charged block copolymer behaves like neutral copolymer. This is because the electrostatic interactions are short ranged in this regime. But there is a remarkable effect of small ions on $\chi_{AB}^* N$ and in fact, it is found that charged block copolymers have to have higher $\chi_{AB}^* N$ as compared to its neutral analog for undergoing the microphase separation. For salty systems,

$$(\chi_{AB}^* N)_{charged} = (\chi_{AB}^* N)_{neutral} + \frac{2\pi l_B Z_A^2 \alpha^2 \rho_0 N}{\kappa^2} \quad (27)$$

For salt-free incompressible system where $\kappa^2 = 4\pi l_B f \alpha Z_c^2 / l^3$, this expression simplifies to

$$(\chi_{AB}^* N)_{charged} = (\chi_{AB}^* N)_{neutral} + \frac{1}{2} \left(\frac{Z_A}{Z_c} \right)^2 \frac{\alpha N}{f} \quad (28)$$

Physically, this means that homogeneous phase in charged copolymer enjoys larger parameter space as compared to its neutral analog.

Case (ii): $r_D \gg D$

In this regime, the structure factor becomes

$$S^{-1}(k) = Bk^2 + \frac{A+C}{k^2} - \bar{\chi} \quad (29)$$

The maxima of the structure factor corresponds to

$$k^* = \left(\frac{A+C}{B} \right)^{1/4} \Rightarrow D = 2\pi \left(\frac{A+C}{B} \right)^{-1/4} \quad (30)$$

so that $\bar{\chi}^* = 2\sqrt{(A+C)B}$. Plugging in expressions for A, B and C

$$D = \frac{2\pi N^{1/2} f^{1/4} (1-f)^{1/4} l}{[108 + 48\pi Z_A^2 (1-f)^2 (f\alpha N)^2 l_B l^2 \rho_0]^{1/4}} \quad (31)$$

$$(\chi_{AB}^* N)_{charged} = \frac{1}{\rho_0 l^3} \left[\frac{s(f)}{4f^2(1-f)^2} + \sqrt{\frac{3}{4f^3(1-f)^3} + \frac{(4\pi l_B l^2 \rho_0)(\alpha N)^2 Z_A^2}{12f(1-f)}} \right] \quad (32)$$

From the expression for D , it is clear that *the period decreases with an increase in the degree of ionization* in this limiting case. Comparing $\chi_{AB}^* N$ for charged and neutral block copolymer cases (Eq. (32) and Eq. (25)), it can be inferred that in this limiting regime also, $(\chi_{AB}^* N)_{charged} > (\chi_{AB}^* N)_{neutral}$ and increases with an increase in α .

Further, it can be shown that the correlation effect of ions (Debye-Hückel theory) is weak as long as $\kappa l_B \ll 1$. This means that all of the above limiting laws for salt-free systems are valid as long as $\kappa l_B \ll 1$.

3. Numerical Calculations for Stability Limit

From here onwards, we consider the salt-free melt. To calculate the stability limit for salt-free melts, inverse temperature dependence of χ_{AB} and l_B is clubbed together by the introduction of a parameter (called reduced temperature²⁸) defined as

$$t = \frac{l}{4\pi\alpha l_B} \quad \text{and} \quad \chi_{AB} = \frac{1}{20\pi t} \quad (33)$$

Having written structure factors in terms of t , the stability limit is calculated using

$$\frac{\delta S^{-1}(k)}{\delta k} \Big|_{k=k^*, t=t^*} = 0 \quad (34)$$

$$S^{-1}(k) \Big|_{k=k^*, t=t^*} = 0 \quad (35)$$

where $S^{-1}(k)$ is given in Eqs. (15 - 18). Solving these equations for t^*

$$t^* = \frac{-L + \sqrt{L^2 - 4PR}}{2P} > 0, \quad (36)$$

where

$$P = 60\pi x^* A(x^*) \quad (37)$$

$$L = 10\pi f N Z_c^2 A(x^*) - 6x^* + 10\pi Z_A^2 \alpha N \quad (38)$$

$$R = -f N Z_c^2 \quad (39)$$

$$A(x^*) = Q(x^*) \quad (40)$$

In writing these equations, we have taken $l = 1$. Function Q appearing in these equations has already been defined in Eq. (17). Using Eq. (34), the wavevector at the stability limit is given by solving the equation

$$\frac{\delta Q(x)}{\delta x} \Big|_{x=x^*} = \frac{6Z_A^2 \alpha N t^*}{(6x^* t^* + f N Z_c^2)^2}. \quad (41)$$

First, Eq. (41) is solved for x^* and then t^* is calculated using Eq. (36). Effect of α and N on the stability limit is shown in Figs. 1 - 2. x^* obtained by using Eq. (41) for different values of N is shown in Fig. 3.

4. Ordered Structures

To derive free energy expressions for different ordered structures, we employ the method used by Leibler¹⁶. Following Leibler, we expand the free energy expression in terms of the order parameter up to fourth order. Taking advantage of the fact that in WSL (near stability limit), important fluctuations in polymer densities are those with the wavevector $k = k^*$, we approximate the order parameter by a sum of plane waves, each having the wavevector $k = k^*$. Using this expression for the order parameter, free energy density becomes

$$\delta F_n = \frac{N(F - F_0)}{\Omega k_B T} = 2Nl^3(\chi_s - \chi)\phi_n^2 - \zeta_n \phi_n^3 + \eta_n \phi_n^4 \quad (42)$$

$$2\chi_s l^3 = Q(x^*) + \frac{Z_A^2 \alpha N l^3}{6x^* t + f N Z_c^2} \quad \text{and} \quad \chi = \chi_{AB} \quad (43)$$

where the value of n corresponds to the morphology being studied. To be specific, $n = 1, 3$ and 6 correspond to lamellar, hexagonally close packed (HCP) cylinder and body centred cubic (BCC) spherical morphology, respectively. Functions Γ_3, Γ_4 and coefficients ζ_n, η_n were calculated by Leibler^{16,17} (summarized in Table I). Further, we have adopted the notation used in Ref.¹⁶ for the arguments of the function Γ_4 . The coefficients have the property that $\eta_1 < \eta_3 < \eta_6$ for all f and specifically, for $f = 1/2$, $\zeta_n = 0$. For all the calculations presented in this paper, these coefficients are evaluated at $k = k^*$.

5. Transition Boundaries

By following the Leibler's procedure¹⁶, the disorder-order transition (DOT) and the order-order transitions (OOT) are studied. Minimizing the free energy density (Eq. (42)) with

respect to the order parameter, equilibrium order parameter and free energy densities are obtained. Results of these minimizations are presented in Table II where γ_n is given by

$$\gamma_n = \left[1 - \frac{64\eta_n}{9\zeta_n^2}(\chi_s - \chi)N \right]^{1/2} \quad (44)$$

In order to determine the morphology that evolves at DOT, the free energy density is equated to zero so that $\chi_n N$ at DOT is found to be

$$\chi_n N = \chi_s N - \frac{\zeta_n^2}{8\eta_n} \quad (45)$$

Using the coefficients ζ_n and η_n , it can be shown that BCC ($n = 6$) gives the lowest value for $\chi_n N$ (or highest value of t). So, the morphology that appears first is BCC. Writing Eq. (45) for DOT in terms of the reduced temperature t , the DOT boundary is given by Eq. (36) where $A(x^*)$ is now given by

$$A(x^*) = Q(x^*) - \frac{\zeta_6^2}{4N\eta_6} \quad (46)$$

Subscript 6 implies that the morphology is sphere ($n = 6$). Similarly, order-order transition boundaries are calculated by equating free energy densities for different morphologies. In general, all the transition boundaries (stability limit, DOT and order-order transitions) are calculated using Eq. (36), where only $A(x^*)$ varies. Mathematical conditions and values of $A(x^*)$ for different transition boundaries are summarized in Table III. Function y appearing in Table III is the solution of Eq. (V-35) in Leibler's work¹⁶. Solving these sets of equations, the morphology diagram can be constructed as discussed in Sec. III.

B. Self-Consistent Field Theory (SCFT)

Although RPA gives a valuable insight into the physics of the problem, it is only a linear response treatment. Strictly, this treatment is valid close to the stability limit of homogeneous phase but far from the limit, RPA calculations are not quantitatively correct^{31,32,37}. To go far away from the stability limit, SCFT has been used extensively in the literature^{36,37,39}. Using standard methods³⁹, self-consistent equations are obtained under the saddle point approximation (see Appendix B).

This numerical technique leads to coupling of full non-linear Poisson-Boltzmann equation with standard modified diffusion equation for the polymer chains. We have solved these

sets of equations using an efficient spectral technique³⁷. While solving these equations, experimentally found inverse dependence of Flory's χ parameter has been exploited by using reduced temperature t (Eq. (33)). We have studied the effect of α on $\chi_{AB}^* N$ and compared with the corresponding RPA calculations. Also, the effect of degree of segregation on the period of lamellar morphology is studied (Fig. 4). Monomer densities, counterion densities and electrostatic potential obtained from SCFT calculations are shown in Figs. 5 - 7, respectively..

III. RESULTS

In the previous section, we have provided the necessary equations to describe the microphase separation. Here, we present results for salt-free charged-neutral diblock melts, by solving the above equations.

A. Stability limit - RPA results

In Figs. 1 and 2, we have drawn the stability limits for charge/neutral block copolymer salt-free melt at different degrees of ionizations for $N = 1000$ and $N = 10,000$, respectively. The critical value of the reduced temperature required to induce microphase separation decreases with an increase in the degree of ionization. This is in qualitative agreement with limiting laws presented in Sec. II A and the already established concept that the effective Flory's χ parameter decreases with an increase in degree of ionization for polyelectrolytes²⁸. Unlike the neutral copolymers, χ and N for polyelectrolytic diblock copolymers are independent parameters that govern the phase behaviour. Also, the stability limit depends on fraction of charged block (f) in an unsymmetric fashion. It is to be noted that these results are in agreement with the results reported by Marko and Rabin³. In Ref.³, temperature dependence of χ parameter was not taken into account and critical parameters were calculated by choosing a fixed value of l_B/l . The method of calculations used by Marko and Rabin was similar to the one presented in Appendix A.

B. Period of lamellar phase ($f = 1/2$)

In RPA, near the stability limit, the period of an ordered structure is approximated by $D = 2\pi/k \simeq 2\pi/k^*$. It is well known that the mean field theory¹⁶ for neutral block copolymer predicts $\chi_{AB}^*N = 10.495$ and $x^* = 3.7852$ at $f = 1/2$. Also, the period shows $1/2$ power law dependence on N in WSL (i.e. $x = \text{constant}$) as long as the wavevector dependence of higher order terms in free energy expression is suppressed^{31,32,37}. Physically, this means that block copolymer chains are obeying the Gaussian statistics for chain conformations. Experimentally, there are deviations from this power law because of chain stretching³⁴. As shown in Fig. 3, same power law dependence is obtained using RPA for polyelectrolytic block copolymers when N is large, but the period ($D \sim \sqrt{N/x^*}$) for a given N is smaller than that for an equivalent neutral copolymer system. This effect has been seen by other researchers also³. The decrease in period with increase in degree of ionization, is explained in Ref.³ by an argument that counterions need to be rearranged on microphase segregation and entropy loss is lower if the length scale of fluctuations for these counterions is smaller. It is to be stressed that lowering of D with α is *not* purely entropic effect. This effect is an outcome of electrostatic screening due to counterions and hence, includes both energetic as well as entropic contributions.

At present, we are not aware of any experimental data on the period of charged-neutral block copolymer. Nevertheless we expect the polyelectrolyte chains to be non-Gaussian and D to deviate strongly from $N^{1/2}$ power law in the case of charged systems. SCFT has been quite successful in predicting the period of ordered structures for neutral copolymers. Expecting that SCFT results are valid for weakly charged polyelectrolyte copolymers, results obtained from SCFT calculations are plotted in Fig. 4 for lamellar phase ($f = 1/2, N = 1000$). Lowermost point in the plots of Fig. 4 corresponds to χ_{AB}^*N . By comparing Fig. 4 with Figs. 1 and 3, it is clear that the RPA calculations for χ_{AB}^*N and x^* , are in good agreement with the corresponding SCFT calculations. Analogous to neutral copolymers, it is found that $N^{1/2}$ power law is not valid for ordered microstructures. In addition the qualitative feature that the period of ordered structures is lower than its neutral analog, is clearly seen in these plots.

C. Counterion distribution

The RPA calculations do not provide counterion distributions. On the other hand, SCFT allows calculations of counterion densities and potential self-consistently. Figs. 5 - 7 show monomer densities for charged block (A), counterion densities, and the electrostatic potential, respectively. The onset of microphase separation leads to creation of monomer and counterion density waves (Figs. 5 and 6) because of the incompatibility between the blocks and coupling between charged monomer (A) and counterions, respectively. From these plots, it can be inferred that in the strong segregation limit ($\chi N \rightarrow \infty$), all the counterions are confined to the charged domains. One of the effects of these density waves in the lamellar phases, is the presence of a potential difference between the charged and neutral domains (Fig. 7) whose magnitude increases with the degree of segregation. For the weakly charged diblock copolymer system studied here, total local charge density is close to zero and it is hard to determine the shape of the charge density wave for the system due to the possible numerical errors. To verify the observation that the effective degree of segregation is reduced because of the electrostatic interactions (RPA calculations), we have plotted monomer densities for neutral and charged block copolymer at the same χN (Fig. 8). These plots clearly confirm that effective degree of segregation is lower for charged copolymer melt and counterions have a tendency to drive the system towards homogeneous phase.

D. Morphology diagram for charged-neutral diblock copolymer

The calculation of morphology diagrams using SCFT is a computationally intensive task because of the vast parameter space for polyelectrolytic systems. To get an idea about transition boundaries, we have used RPA calculations presented in section II A, assuming that only the classical morphologies¹⁶ compete in charged-neutral diblock copolymer systems. Figs. 9 and 10 show the calculated morphology diagrams for different α and N . We observe that DOT and OOT boundaries are strongly dependent on α and N . The temperature of occurrence of DOT decreases with an increase in α and increases with an increase in N (analogous to the shift of stability limit - Figs. 1, 2). Furthermore, these transition boundaries for DOT and OOT are highly asymmetric with respect to f .

IV. CONCLUSIONS

We have addressed the microphase separation in charged-neutral diblock copolymer melts in the weak segregation limit, by using the RPA and SCFT methods. We have shown in Sections II A and III that the critical value of the χ parameter for microphase separation is higher for charged copolymers and of concentration modulation is smaller in comparison with neutral copolymers. From morphology diagrams, it can be seen that the parameter space for ordered microstructures is reduced when degree of ionization of charged block is increased. In other words, charging a block stabilizes the homogeneous phase.

The SCFT results show that the counterions partition themselves preferentially within the charged domains. This leads to creation of a potential difference between charged and neutral domains. This process of partitioning is unfavorable both entropically and energetically. Hence, the length scale of these partitioning is lower when there are more number of counterions to be partitioned for the same number of monomers.

Finally, we summarize the assumptions in obtaining the above results. We have taken the counterions to be point charges. Our treatment can be readily extended to counterions with finite size by modifying the incompressibility condition and incorporating excluded volume interactions. The Kuhn segment lengths for the neutral and charged blocks are taken to be same. It has been shown that conformational asymmetry has an effect on the order-order transition boundaries for neutral copolymers³⁸. Analogously, there will be an effect on our system as well. In the case of polyelectrolytes, electrostatic interactions cause stiffening of the chain so that the effective segment length²⁶ depends on various factors such as κ , α etc. in a complicated manner. By assuming that the segment length for charged and neutral blocks to be the same, we implicitly assume that the charged block copolymer under consideration is conformationally symmetric and is weakly charged, so that the difference between the effective and bare segment lengths is negligible. Another important assumption in the present theory is that the position/concentration dependence of the dielectric constant ϵ is suppressed. Recently, the effect of dielectric constants of individual components in a multi-component polyelectrolyte³⁶ solution has been presented. In this work, dielectric constant of a component was taken to be linearly dependent on the concentration of the component. In principle, dielectric constant depends on the concentration of ions in a complex manner⁴⁰. At present, there is no satisfactory well-established model for the dependence of microscopic

dielectric constant on macroscopic density. So, we model dielectric constant (ϵ) appearing in the expression for the Bjerrum length as the effective dielectric constant for the mixture of A, B monomers and counterions. Position dependence of dielectric constant will definitely play an important role in the strong segregation limit. However, for melts in WSL, the average value of dielectric constant can be taken as a constant. Further, we have considered only the lamellar, cylindrical and spherical morphologies as the competing structures. Extensions of the present theory for other morphologies are in progress.

At present we are unaware of any systematic experimental study on charged-neutral copolymer. We hope that the present theoretical work will instigate experimental work on charged block copolymers in the concentrated regime.

ACKNOWLEDGEMENT

We acknowledge financial support from the National Science Foundation (Grant No. DMR-0605833) and the Materials Research Science and Engineering Centre at the University of Massachusetts, Amherst. We are also grateful to Dr. Chilun Lee for discussions.

APPENDIX A : Integration over positions of small ions

Here, we present how to compute the integral over positions of small ions. If microscopic charge density at any point in space is defined as

$$\hat{\rho}_e(r) = e \left[Z_A \alpha \hat{\rho}_A(r) + \sum_{m=c,+,-} Z_m \hat{\rho}_m(r) \right] \quad (\text{A-1})$$

where $\hat{\rho}_A(r)$ is given by Equation 8 and charge density of small ions is defined as

$$\hat{\rho}_m(r) = \sum_{i=1}^{n_m} Z_m \delta(r - r_i). \quad (\text{A-2})$$

Using these definitions of densities, Equation 1 can be written in the form

$$\begin{aligned} \exp\left(-\frac{F}{k_B T}\right) = & \frac{1}{n! n_c! \prod_{\gamma} n_{\gamma}} \int \prod_{j=1}^n D[R_j] \int \prod_{i=1}^{n_c + \sum_{\gamma} n_{\gamma}} dr_i \exp \left[-\frac{3}{2l} \sum_{j=1}^n \int_0^{Nl} ds_j \left(\frac{\partial R_j}{\partial s_j} \right)^2 \right. \\ & \left. - l^3 \int dr \chi_{AB} \hat{\rho}_A(r) \hat{\rho}_B(r) - \frac{1}{2} \int dr \int dr' \frac{\hat{\rho}_e(r) \hat{\rho}_e(r')}{\epsilon k_B T |r - r'|} \right] \\ & \prod_r \delta[\hat{\rho}_A(r) + \hat{\rho}_B(r) - \rho_0]. \end{aligned} \quad (\text{A-3})$$

Here, χ_{AB} is Flory's chi parameter, which accounts for chemical mismatch between blocks and is defined as

$$\chi_{AB}l^3 = w_{AB} - \frac{w_{AA} + w_{BB}}{2} \quad (\text{A-4})$$

Terms corresponding to excluded volume interactions can be treated in the usual way³⁹. Here we present the treatment of electrostatic terms. We introduce field variables to go from particles to fields by defining $\hat{\phi}_p(r) = \frac{\hat{\rho}_p(r)}{\rho_0}$ where $p = A, B, c, +, -$ (i.e. p corresponds to all components in system i.e. A -block, B -block, counterions and coions). Before proceeding, we introduce the identity

$$1 = \int D[\phi_p(r)] \prod_r \delta\{\phi_p(r) - \hat{\phi}_p(r)\} \quad (\text{A-5})$$

$$= \int D[\phi_p(r)] \int D[w_p(r)] \exp \left[i\rho_0 \int dr w_p(r) \{\phi_p(r) - \hat{\phi}_p(r)\} \right]. \quad (\text{A-6})$$

Here, i is purely imaginary number and to avoid confusion, we are going to use the notation $iw_p(r) \rightarrow w_p(r)$ for all purely imaginary fields. In this notation, Equation A-3 can be written in the form

$$\exp \left(-\frac{F}{k_B T} \right) = \int \prod_p D[\phi_p(r)] D[w_p(r)] D[\eta(r)] \exp \left[-\frac{H}{k_B T} \right] \quad (\text{A-7})$$

$$\begin{aligned} \exp \left(-\frac{H}{k_B T} \right) &= \frac{\tau^n \Omega^{n_c + \sum_\gamma n_\gamma}}{n! n_c! \prod_\gamma n_\gamma} \exp \left[-l^3 \rho_0^2 \int dr \chi_{AB} \phi_A(r) \phi_B(r) - \frac{\rho_0^2}{2} \int dr \int dr' \frac{\rho_e(r) \rho_e(r')}{\epsilon k_B T |r - r'|} \right. \\ &\quad \left. + \rho_0 \int dr \left\{ \sum_p w_p(r) \phi_p(r) + \eta(r) (\phi_A(r) + \phi_B(r) - 1) \right\} \right] Q_{AB}^n Q_c^{n_c} Q_+^{n_+} Q_-^{n_-} \end{aligned} \quad (\text{A-8})$$

where $i\eta(r) \rightarrow \eta(r)$ is the field introduced to enforce the incompressibility condition at all points and

$$\rho_e(r) = e \left[Z_A f \alpha \phi_A(r) + \sum_{m=c,+, -} Z_m \phi_m(r) \right] \quad (\text{A-9})$$

$$Q_{AB} = \frac{1}{\tau} \int D[R] \exp \left[-\frac{3}{2l} \int_0^{Nl} ds \left(\frac{\partial R(s)}{\partial s} \right)^2 - \frac{1}{l} \int_0^{N_A l} ds w_A(R(s)) - \frac{1}{l} \int_{N_A l}^{Nl} ds w_B(R(s)) \right] \quad (\text{A-10})$$

$$Q_i = \frac{1}{\Omega} \int dr \exp [-w_i(r)] \quad (\text{A-11})$$

Here, subscript $i (= c, +, -)$ corresponds to all kinds of small ions in the system. Ω is the total volume and τ is a normalization constant given by

$$\tau = \int D[R] \exp \left[-\frac{3}{2l} \int_0^M ds \left(\frac{\partial R(s)}{\partial s} \right)^2 \right] \quad (\text{A-12})$$

Integrals over w_p can't be calculated exactly. So, in order to proceed further, integrals over $w_i(r)$ are approximated by the maximum value of the integrand (saddle point approximation). Maximization of the integrand with respect to $w_i(r)$ gives

$$\phi_i(r) = \frac{n_i}{\rho_0 \Omega Q_i} \exp [-w_i(r)] \Rightarrow w_i(r) = -\ln \left[\frac{\rho_0 \Omega Q_i}{n_i} \right] - \ln [\phi_i(r)] \quad (\text{A-13})$$

Plugging w_i back into Eq. (A-7),

$$\exp \left(-\frac{F}{k_B T} \right) = \int \prod_p D[\phi_p(r)] D[w_A(r)] D[w_B(r)] D[\eta(r)] \exp \left[-\frac{H^*}{k_B T} \right] \quad (\text{A-14})$$

$$\begin{aligned} \exp \left(-\frac{H^*}{k_B T} \right) &= \frac{\tau^n (\rho_0)^{-n_c - \sum_\gamma n_\gamma}}{n! n_c! \prod_\gamma n_\gamma} \exp \left[-l^3 \rho_0^2 \int dr \chi_{AB} \phi_A(r) \phi_B(r) \right. \\ &\quad - \frac{\rho_0^2}{2} \int dr \int dr' \frac{\rho_e(r) \rho_e(r')}{\epsilon k_B T |r - r'|} + \rho_0 \int dr w_A(r) \phi_A(r) \\ &\quad + \rho_0 \int dr w_B(r) \phi_B(r) - \rho_0 \int dr \sum_{i=c,+} \phi_i(r) \ln [\phi_i(r)] \\ &\quad \left. + \rho_0 \int dr \eta(r) \{ \phi_A(r) + \phi_B(r) - 1 \} \right] Q_{AB}^n. \end{aligned} \quad (\text{A-15})$$

In order to calculate the integral over ϕ_i , we consider fluctuations of charge densities about the disordered phase³. For weak fluctuations, the entropic term $\phi_i \ln \phi_i$ can be expanded in powers of these fluctuations. Keeping the leading terms (neglecting cubic and higher order terms), integrals over ϕ_i become Gaussian and can be easily calculated. So, by writing

$$\phi_i(r) = \langle \phi_i \rangle + \delta \phi_i(r) \quad (\text{A-16})$$

, and using $\int dr \delta \phi_i(r) = 0$ in combination with the global electroneutrality in the homogeneous phase, integrals over ϕ_i (i.e. small ions) become

$$\begin{aligned} I &= \int \prod_{m=1}^3 D[\delta \phi_m] \exp \left[-\frac{\rho_0^2}{2} \int \frac{d^3 k}{(2\pi)^3} \left\{ \sum_{m=1}^3 \sum_{q=1}^3 \delta \phi_m(k) \left(\frac{\delta_{mq}}{\rho_0 \langle \phi_m \rangle} + V_k^{(0)} Z_m Z_q \right) \delta \phi_q(k) \right. \right. \\ &\quad \left. \left. + 2 \sum_{m=1}^3 V_k^{(0)} \alpha Z_A Z_m \delta \phi_A(k) \delta \phi_m(k) \right\} \right] \exp \left[-\frac{\rho_0^2}{2} \int \frac{d^3 k}{(2\pi)^3} V_k^{(0)} \alpha^2 Z_A^2 \delta \phi_A^2(k) \right], \end{aligned} \quad (\text{A-17})$$

where $V_k^{(0)} = \frac{4\pi l_B}{k^2}$, δ_{mp} is the Kronecker delta and the indices 1,2,3 correspond to counterion from polymer, positive (+) and negative (-) salt ions, respectively. By calculating the Gaussian integrals, the value of I is found to be

$$I = \frac{(2\pi)^{\frac{3}{2}}}{\rho_0^3 \sqrt{c_1 c_2 c_3}} \exp \left[-\frac{\Omega}{2} \int \frac{d^3 k}{(2\pi)^3} \ln \left[1 + V_k^{(0)} c_0 \right] \right] \exp \left[-\frac{\rho_0^2}{2} \alpha^2 Z_A^2 \int \frac{d^3 k}{(2\pi)^3} \frac{V_k^{(0)}}{1 + V_k^{(0)} c_0} \delta \phi_A^2(k) \right] \quad (\text{A-18})$$

where $c_m = \frac{\Omega}{n_m}$ and c_0 is given by

$$c_0 = \frac{1}{\Omega} \sum_{m=1,2,3} Z_m^2 n_m = \frac{\kappa^2}{4\pi l_B} \quad (\text{A-19})$$

Now, using the relation

$$\int_0^\infty x^2 \left\{ \ln \left[1 + \frac{\alpha^2}{x^2} \right] - \frac{\alpha^2}{x^2} \right\} = -\frac{\pi}{3} \alpha^3, \quad (\text{A-20})$$

we get

$$\frac{\Omega}{2} \int \frac{d^3 k}{(2\pi)^3} \ln(1 + c_0 V_k^{(0)}) = -\frac{\Omega}{12\pi} (4\pi l_B c_0)^{3/2} + \frac{\Omega}{2} \int \frac{d^3 k}{(2\pi)^3} \frac{4\pi l_B c_0}{k^2} \quad (\text{A-21})$$

Here, the last term is divergent. But the divergence is for k being large (ultraviolet divergence) and we are interested on a length scale corresponding to small k . So, this term is neglected. Note that the same result can be obtained by employing the central limit theorem²⁷. Now, electrostatic terms are decoupled from the rest of the terms and remaining treatment is the same as that done for the corresponding neutral copolymer¹⁹.

APPENDIX B : Self-Consistent Field Theory

Instead of expanding about average densities, the introduction of another field corresponding to charge density^{35,36} in Eq. (A-7), leads to the following self consistent equations for the *salt-free melt* after taking $l = 1$

$$\chi_{AB} N \phi_B(r) = w_A(r) + \eta(r) \quad (\text{B-1})$$

$$\chi_{AB} N \phi_A(r) = w_B(r) + \eta(r) \quad (\text{B-2})$$

$$\phi_A(r) + \phi_B(r) = 1 \quad (\text{B-3})$$

$$\phi_C(r) = -\frac{Z_A f \alpha}{Z_c Q_c} \exp[-Z_c \psi(r)] \quad (\text{B-4})$$

$$\phi_A(r) = \frac{\Omega \int_0^f ds q(r, s) q^*(r, 1-s)}{\int dr q(r, 1)} \quad (\text{B-5})$$

$$\phi_B(r) = \frac{\Omega \int_f^1 ds q(r, s) q^*(r, 1-s)}{\int dr q(r, 1)} \quad (\text{B-6})$$

$$\nabla_r^2 \psi(r) = -4\pi l_B [Z_c \phi_C(r) + Z_A \alpha \phi_A(r)] \quad (\text{B-7})$$

$$\frac{\partial q(r, s)}{\partial s} = \begin{cases} \left[\frac{N}{6} \nabla_r^2 - \{Z_A \alpha N \psi(r) + w_A(r)\} \right] q(r, s) & s \leq f \\ \left[\frac{N}{6} \nabla_r^2 - w_B(r) \right] q(r, s) & s \geq f \end{cases} \quad (\text{B-8})$$

$$\frac{\partial q^*(r, t)}{\partial t} = \begin{cases} \left[\frac{N}{6} \nabla_r^2 - \{Z_A \alpha N \psi(r) + w_A(r)\} \right] q^*(r, t) & t \geq (1-f) \\ \left[\frac{N}{6} \nabla_r^2 - w_B(r) \right] q^*(r, t) & t \leq (1-f) \end{cases} \quad (\text{B-9})$$

These equations are to be solved with initial conditions $q(r, 0) = 1$, $q^*(r, 0) = 1$ and the free energy expression for the salt-free melt (per chain) becomes

$$\begin{aligned} \frac{F}{nk_B T} = & -\frac{1}{\Omega} \int dr \chi_{AB} N \phi_A(r) \phi_B(r) - \frac{N}{8\pi l_B \Omega} \int dr |\nabla_r \psi(r)|^2 + \frac{1}{\Omega} \int dr \eta(r) \\ & - \left\{ \ln \left[\frac{Q_{AB}}{n} \right] - \frac{Z_A f \alpha N}{Z_c} \ln \left[\frac{Q_c}{n_c} \right] - \frac{Z_A f \alpha N}{Z_c} (\ln \Omega + 1) + (\ln \tau + 1) \right\} \end{aligned} \quad (\text{B-10})$$

Here, we have used the notation $ie\psi(r) \rightarrow \psi(r)$ for purely imaginary electrostatic potential and $iw_p(r) \rightarrow w_p(r)$ for all the purely imaginary fields. Expressions for Q_c , Q_{AB} and τ are given in Appendix A. The free energy of the homogeneous phase (where all the densities and fields are constant) is given by

$$\frac{F}{nk_B T} = \chi_{AB} N f (1-f) + \left(-\frac{Z_A}{Z_c} f \alpha N \right) \left\{ \ln \left[-\frac{Z_A}{Z_c} f \alpha \right] - 1 \right\} \quad (\text{B-11})$$

REFERENCES

- ¹ A.R. Khokhlov, J.Phys.A: Math. Gen.,13, 979 (1980).
- ² V.Yu. Borue and I.Ya. Erukhimovich, Macromolecules, 21, 3240 (1988).
- ³ (a) J.F. Marko and Y. Rabin , Macromolecules, 24, 2134 (1991); (b) *ibid.* 25, 1503 (1992);
- ⁴ M. Benmouna, T.A. Vilgis and J. François, Makromol. Chem.,Theory Simul., 1, 3 (1992).
- ⁵ M. Benmouna and Y. Bouayed, Macromolecules, 25, 5318 (1992).
- ⁶ E.E. Dormidontova, I. Ya. Erukhimovich and A.R. Khokhlov, Macromol. Theory and Simul., 3, 661 (1994).
- ⁷ G.A. Carri and M. Muthukumar, J. Chem. Phys., 111, 1765 (1999).
- ⁸ K. Ghosh, G.A. Carri and M. Muthukumar, J. Chem. Phys., 116, 5299 (2002).
- ⁹ K. Nishida, K. Kaji and T. Kanaya, J. Chem. Phys., 114, 8671 (2001).
- ¹⁰ K. Nishida, K. Kaji and T. Kanaya, J. Chem. Phys., 115, 8217 (2001).
- ¹¹ K. Yu and A. Eisenberg, Macromolecules,31, 3509 (1998).
- ¹² S.A. Jenekhe and X.L. Chen, Science, 279, 1903 (1998).
- ¹³ X.L. Chen and S.A. Jenekhe, Langmuir, 15, 8007 (1999).
- ¹⁴ T. Nakanishi, S. Fukushima, K. Okamoto, M. Suzuki, Y. Matsumara, M. Yokoyama, T. Okano, Y. Sakurai and K. Kataoka, J. Control. Release, 74, 295 (2001).
- ¹⁵ (a) E. Helfand, J. Chem. Phys. 62, 999 (1975);(b) Macromolecules,8, 552 (1975);(c) *ibid.* 9, 879 (1976);(d) *ibid.* 11, 960 (1978);(e) *ibid.* 13, 994 (1980).
- ¹⁶ L. Leibler, Macromolecules, 13, 1602 (1980).
- ¹⁷ There are few misprints in Ref.¹⁶. Corrections are:

(1) Equation (V-33) should read

$$\gamma_n = [3a_n + 1 + 2(3a_n + 1)^{1/2}]/3(a_n - 1)$$

(2) Equation (C-6) should read

$$g_4(f, h) = \{1 - \exp[-(1 - f)x]\}\{1 + \exp(-hfx)/(h - 1) - h \exp(-fx)/(h - 1)\}/hx^3$$

(3) In Appendix C, functions $g_i(f, h)$ and $f_i(f, h)$ where $i = 2, 3, 4$, are defined and these functions have special cases for $h = 0, 1, 3, 4$. In fact, these functions differ from general expres-

- sions (like Eq. (C-4)) only for $h = 0, 1$ and for all other values of h , general expressions are true. So, equations like (C-4a) and (C-4b) are valid *only* for $h = 0$ and $h = 1$ respectively.
- ¹⁸ (a) A.N. Semenov, Zh. Eksp. Teor. Fiz., 88, 1242 (1985); (b) Macromolecules, 22, 2849 (1989).
- ¹⁹ (a) T. Ohta and K. Kawasaki, Macromolecules, 19, 2621 (1986); (b) *ibid.* 21, 2972 (1988); (c) *ibid.* 23, 2413 (1990).
- ²⁰ (a) E.B. Zhulina and O.V. Borisov, Macromolecules, 35, 9191(2002); (b) O.V. Borisov and E.B. Zhulina, *ibid.*, 35, 4472(2002); (c) *ibid.*, 36, 10029(2003).
- ²¹ N. Dan and M. Tirrell, Macromolecules, 26, 4310 (1993).
- ²² N.P. Shusharina, I.A. Nyrkova and A.R. Khokhlov, Macromolecules, 29, 3167 (1996).
- ²³ I.A. Nyrkova and A.N. Semenov, Faraday Discuss., 128, 113(2005).
- ²⁴ A.V. Kyrylyuk and J.G.E.M. Fraaije, J. Chem. Phys., 121, 2806(2004).
- ²⁵ A.V. Kyrylyuk and J.G.E.M. Fraaije, J. Chem. Phys., 121, 9166(2004).
- ²⁶ M. Muthukumar, J. Chem. Phys., 86, 7230 (1987).
- ²⁷ M. Muthukumar, J. Chem. Phys., 105, 5183 (1996).
- ²⁸ M. Muthukumar, Macromolecules, 35, 9142 (2002).
- ²⁹ G.H. Fredrickson and E. Helfand, J. Chem. Phys., 87, 697 (1987).
- ³⁰ M. Olvera de la Cruz, Phys. Rev. Lett., 67, 85 (1991).
- ³¹ J. Melenkevitz and M. Muthukumar, Macromolecules, 24, 4199 (1991).
- ³² R.L. Lescanec and M. Muthukumar, Macromolecules, 26, 3908 (1993).
- ³³ M. Muthukumar, Macromolecules, 26, 5259 (1993).
- ³⁴ K. Almdal, J. H. Rosedale, F. Bates, G. D. Wignall and G. H. Fredrickson, Phys. Rev. Lett., 65, 1112 (1990).
- ³⁵ A. Shi and J. Noolandi, Macromol. Theory Simul., 8, 214 (1999).
- ³⁶ (a) Q. Wang, T. Taniguchi and G.H. Fredrickson, J. Phys. Chem. B, 108, 6733 (2004); (b) *ibid.* 109, 9855 (2005).
- ³⁷ (a) M.W. Matsen and M. Schick, Phys. Rev. Lett., 72, 2660 (1994); (b) M.W. Matsen and F.S. Bates, Macromolecules, 29, 1091 (1996); (c) M.W. Matsen, J. Phys.: Condens. Matter 14, R21 (2002).
- ³⁸ (a) J. D. Vavasour and M. D. Whitmore, Macromolecules 25, 5477 (1992); (b) M.W. Matsen and F.S. Bates, J. Polym. Sci. B: Polym. Phys. 35, 945 (1997);
- ³⁹ G.H. Fredrickson, *The Equilibrium Theory of Inhomogeneous Polymers* (Oxford University, New

York, 2006).

⁴⁰ C.J.F. Böttcher, *Theory of Electric Polarization* (Elsevier, Amsterdam, 1973).

FIGURE CAPTION

- Fig. 1.:** Effect of degree of ionization (α) on the stability limit in polyelectrolytic diblock melt: plots correspond to $N = 1000$ and $\alpha = 0, 0.01, 0.02, 0.1$.
- Fig. 2.:** Effect of degree of ionization (α) on the stability limit in polyelectrolytic diblock melt: plots correspond to $N = 10,000$ and $\alpha = 0, 0.01, 0.02, 0.1$.
- Fig. 3.:** RPA Calculations - Effect of degree of polymerization (N) and degree of ionization (α) on critical parameter x^* for ($f = \frac{1}{2}$) in WSL : $\alpha = 0, 0.01, 0.02, 0.1$.
- Fig. 4.:** SCFT Calculations - Effect of degree of segregation on period of lamellae ($f = 1/2, N = 1000$). Semenov's Strong Segregation Theory (SSST)^{18,37} which predicts $D/(N^{1/2}l) = 2(8\chi N/3\pi^4)^{1/6}$ is also drawn for comparison purposes.
- Fig. 5.:** Polyelectrolytic block copolymer lamellae ($f = 1/2, \alpha = 0.01, N = 1000$) - monomer densities.
- Fig. 6.:** Counterion distribution in lamellar phase ($f = 1/2, \alpha = 0.01, N = 1000$).
- Fig. 7.:** Electrostatic potential in lamellar phase ($f = 1/2, \alpha = 0.01, N = 1000$).
- Fig. 8.:** Reduction of effective chemical mismatch ($f = 1/2, N = 1000$) - comparison between monomer densities.
- Fig. 9.:** RPA Calculations - Morphology diagram for polyelectrolytic diblock copolymer: $N = 1000$ and $\alpha = 0$ for the topmost four boundaries, $\alpha = 0.01$ for the middle four, $\alpha = 0.02$ for the next set and $\alpha = 0.1$ for the lowermost four boundaries.
- Fig. 10.:** RPA Calculations - Morphology diagram for polyelectrolytic diblock copolymer: $N = 10,000$ and $\alpha = 0$ for the topmost four boundaries, $\alpha = 0.01$ for the middle four, $\alpha = 0.02$ for the next set and $\alpha = 0.1$ for the lowermost four boundaries.

Morphology	ζ_n	η_n
Lamellar	$\zeta_1 = 0$	$\eta_1 = \frac{N}{4}\Gamma_4(0, 0)$
Cylinder	$\zeta_3 = -(2/3\sqrt{3})N\Gamma_3$	$\eta_3 = \frac{N}{12}(\Gamma_4(0, 0) + 4\Gamma_4(0, 1))$
Sphere	$\zeta_6 = -(4/3\sqrt{6})N\Gamma_3$ $+2\Gamma_4(0, 2) + 4\Gamma_4(1, 2)$	$\eta_6 = \frac{N}{24}(\Gamma_4(0, 0) + 8\Gamma_4(0, 1)$

TABLE I: Coefficients ζ_n and η_n calculated by Leibler¹⁶

Morphology	Order Parameter ($\bar{\phi}_n$)	Free Energy Density (δF_n)
Disorder - Order Transition	$\zeta_n / (2\eta_n)$	0
Lamellar	$\sqrt{(\chi - \chi_s)N/\eta_1}$	$-N^2(\chi_s - \chi)^2/\eta_1$
Sphere, Cylinder	$3\zeta_n(1 + \gamma_n) / (8\eta_n)$	$27\zeta_n^4(1 + \gamma_n)^3(1 - 3\gamma_n) / (4096\eta_n^3)$

TABLE II: Equilibrium order parameters and free energy densities

Transition Boundary	Mathematical Conditions	$A(x^*)$
Stability Limit	$\frac{\delta S^{-1}(k)}{\delta k} \Big _{k=k^*, t=t^*} = 0$ $S^{-1}(k) \Big _{k=k^*, t=t^*} = 0$	$Q(x^*)$
Disorder - Order	$\frac{\partial(\delta F_n)}{\partial \phi_n} \Big _{\phi_n=\bar{\phi}_n} = 0$ $\frac{\partial^2(\delta F_n)}{\partial \phi_n^2} \Big _{\phi_n=\bar{\phi}_n} > 0$ $\delta F_n(\bar{\phi}_n, t_n) = 0$	$Q(x^*) - \zeta_6^2 / (4N\eta_6)$
Sphere - Cylinder	$\delta F_6 = \delta F_3$	$Q(x^*) + 2y/N$
Cylinder - Lamellar	$\delta F_3 = \delta F_1$	$Q(x^*) + 9\zeta_3^2(\gamma_3^2 - 1) / (32N\eta_3)$

TABLE III: Description of different transition boundaries

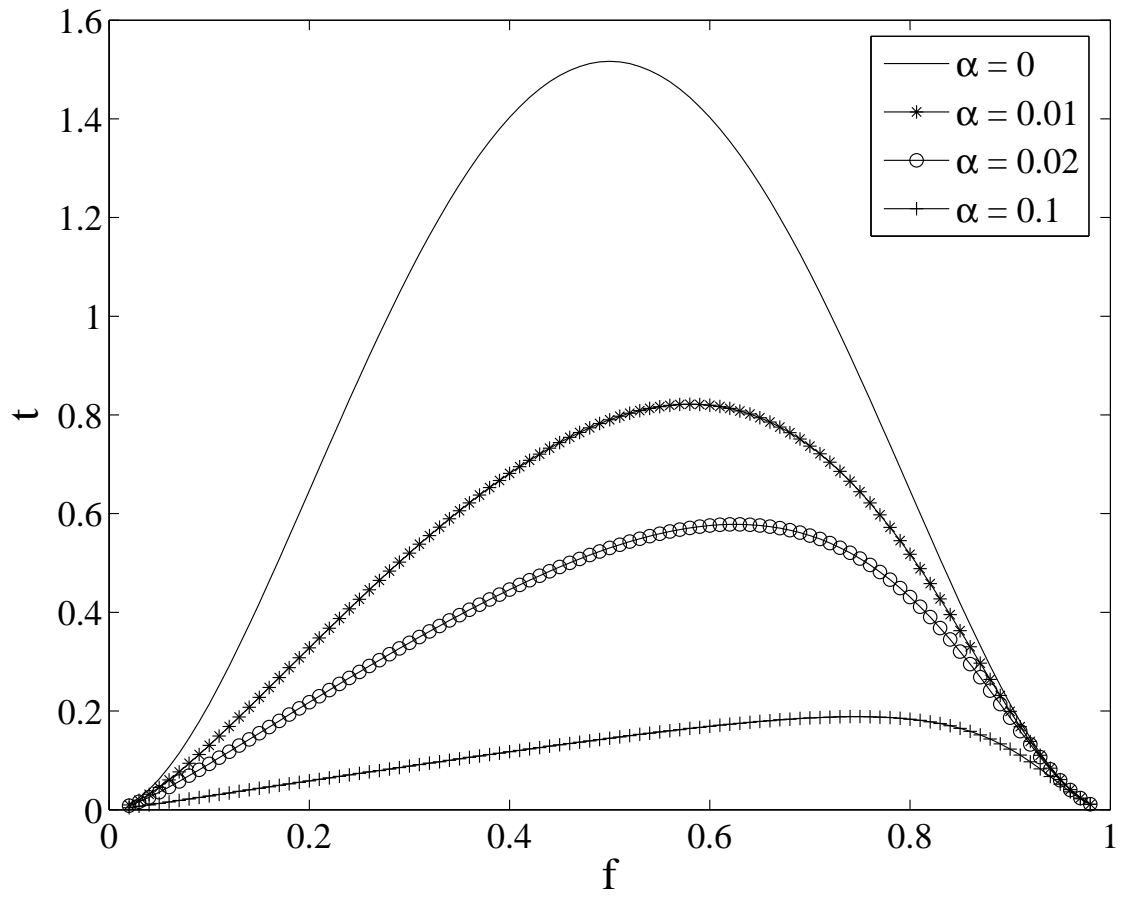


FIG. 1:

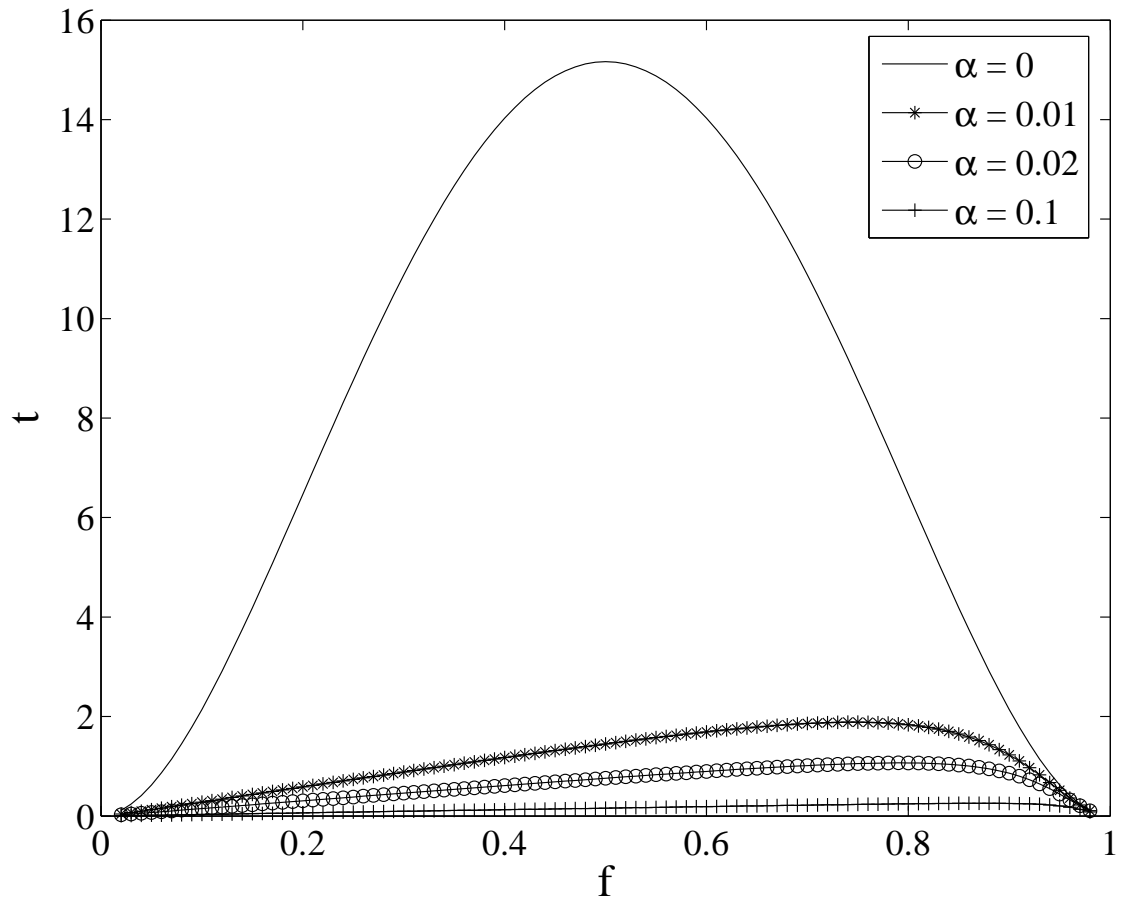


FIG. 2:

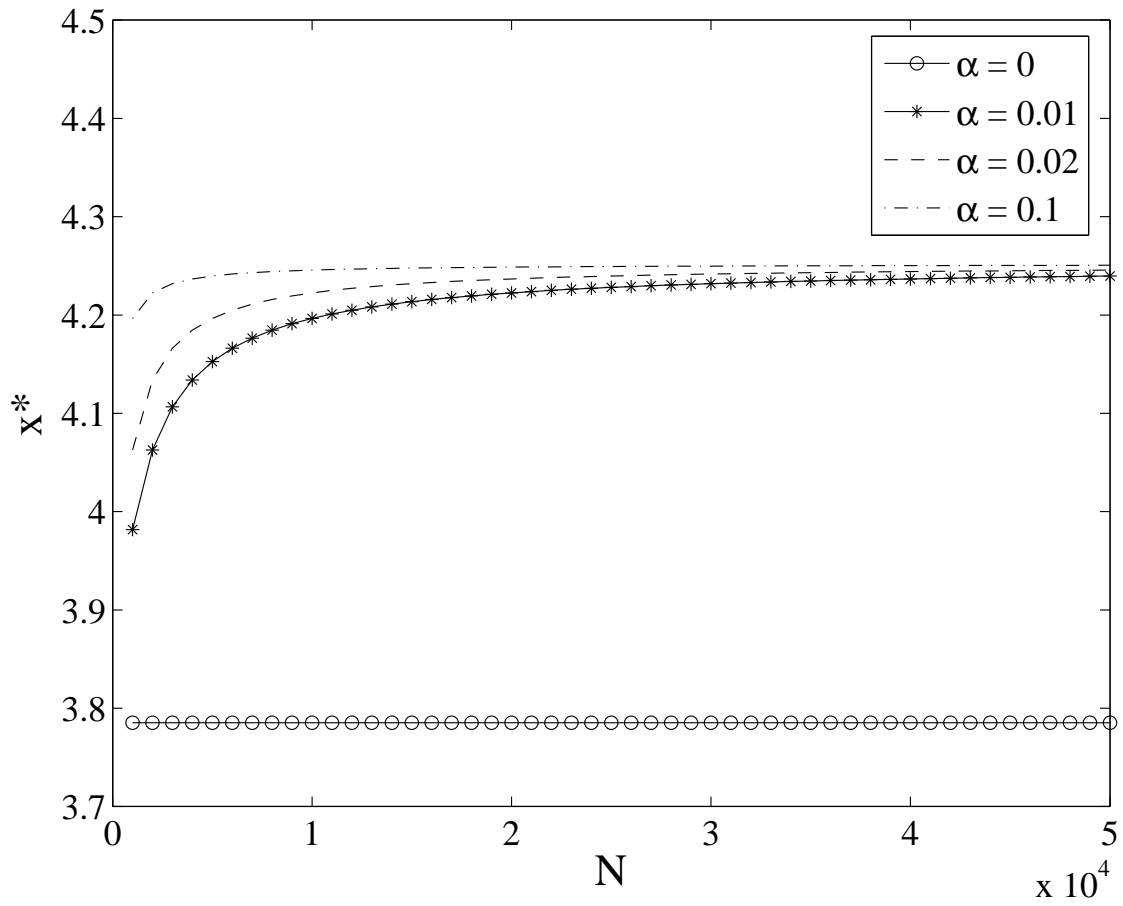


FIG. 3:

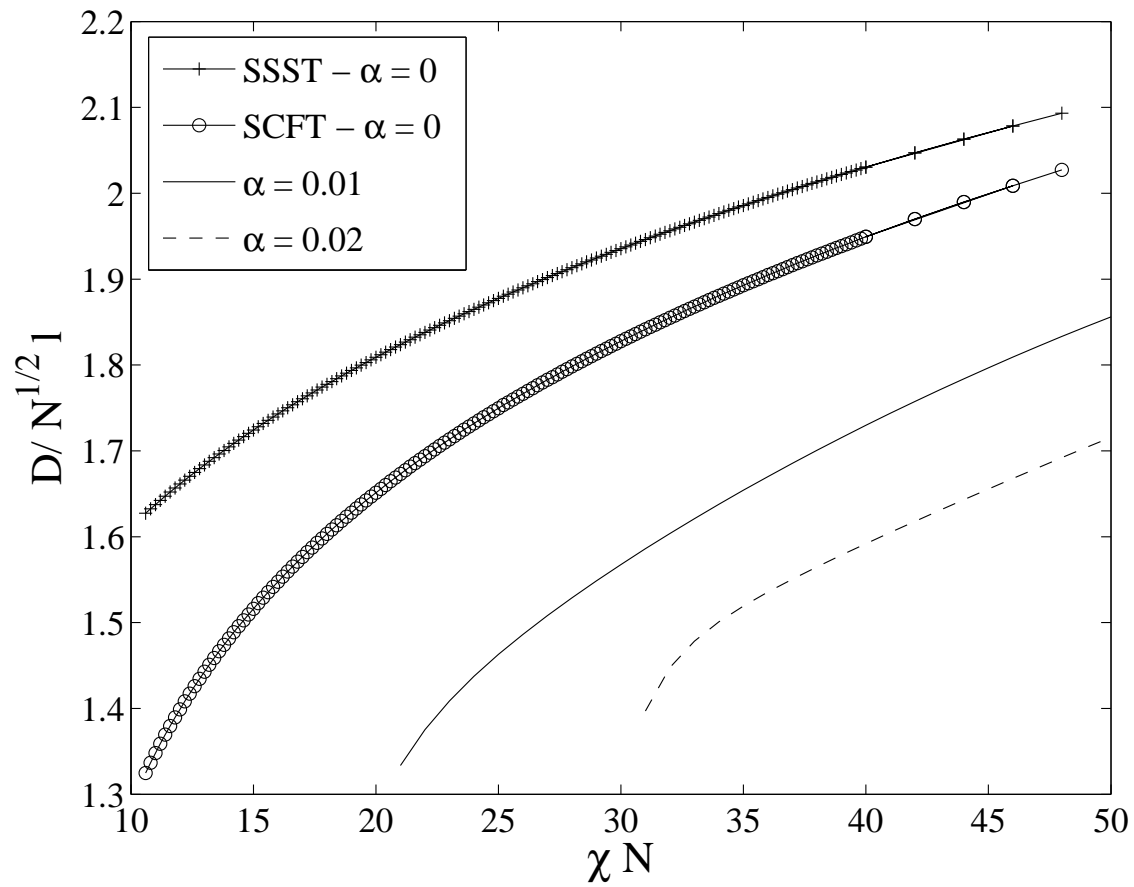


FIG. 4:

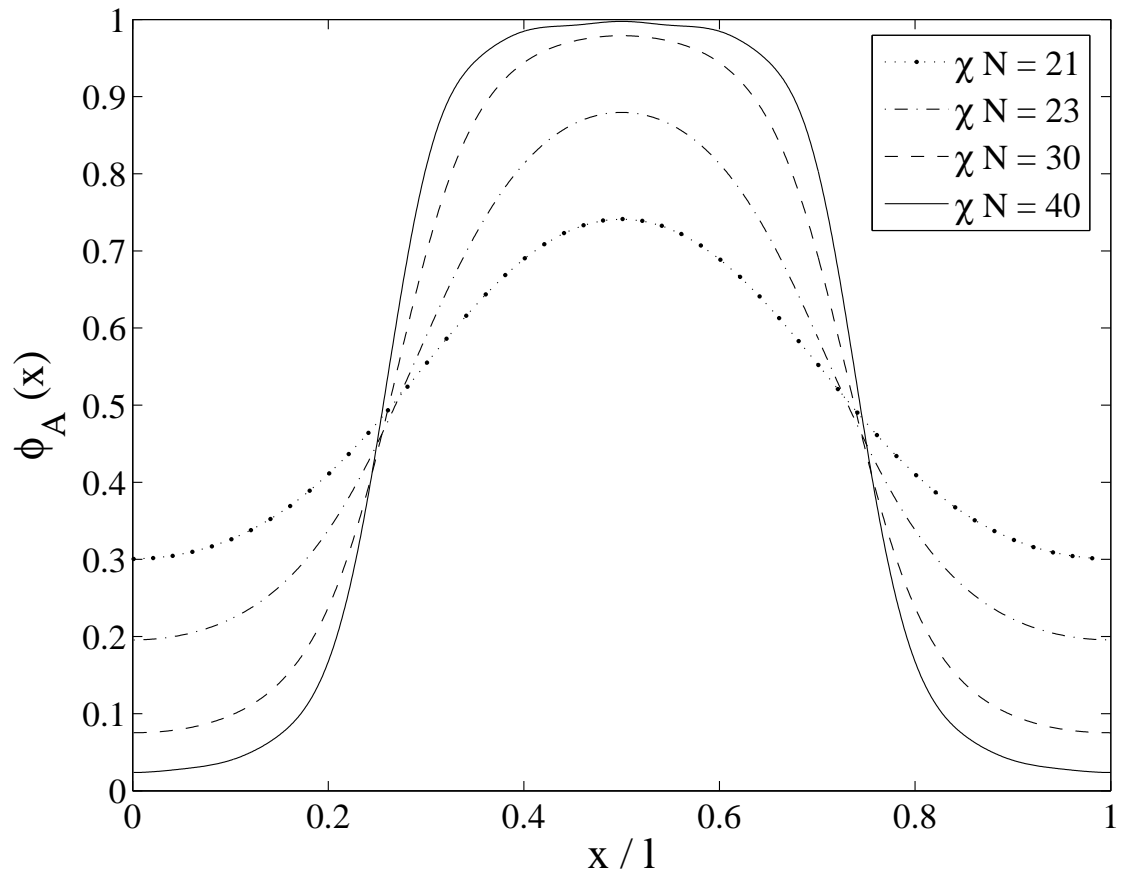


FIG. 5:

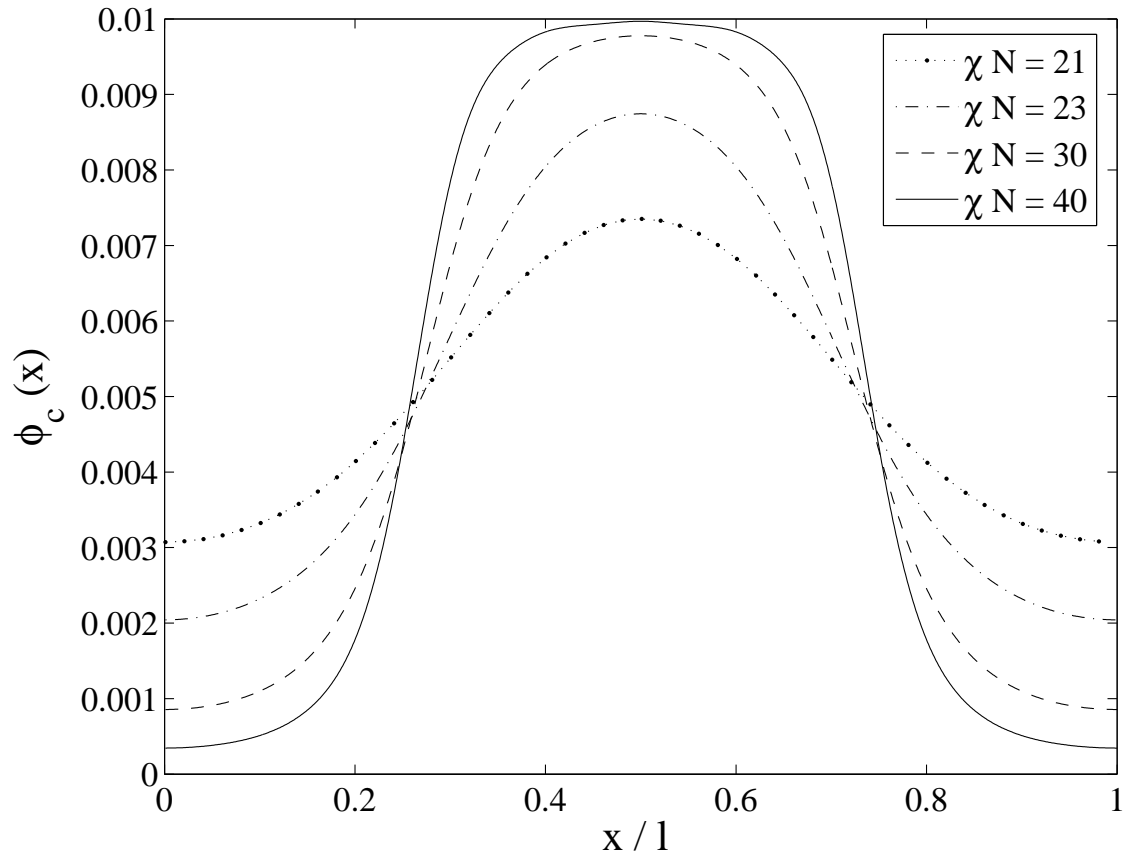


FIG. 6:

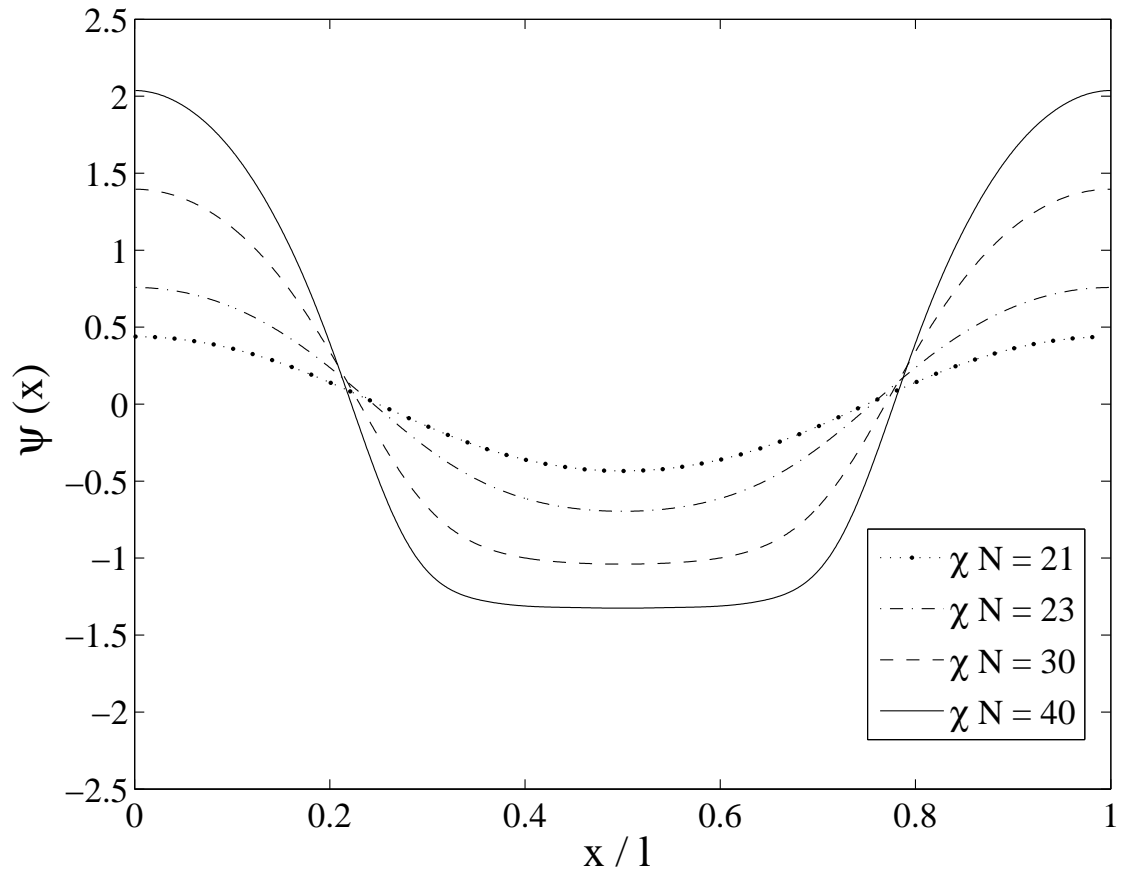


FIG. 7:

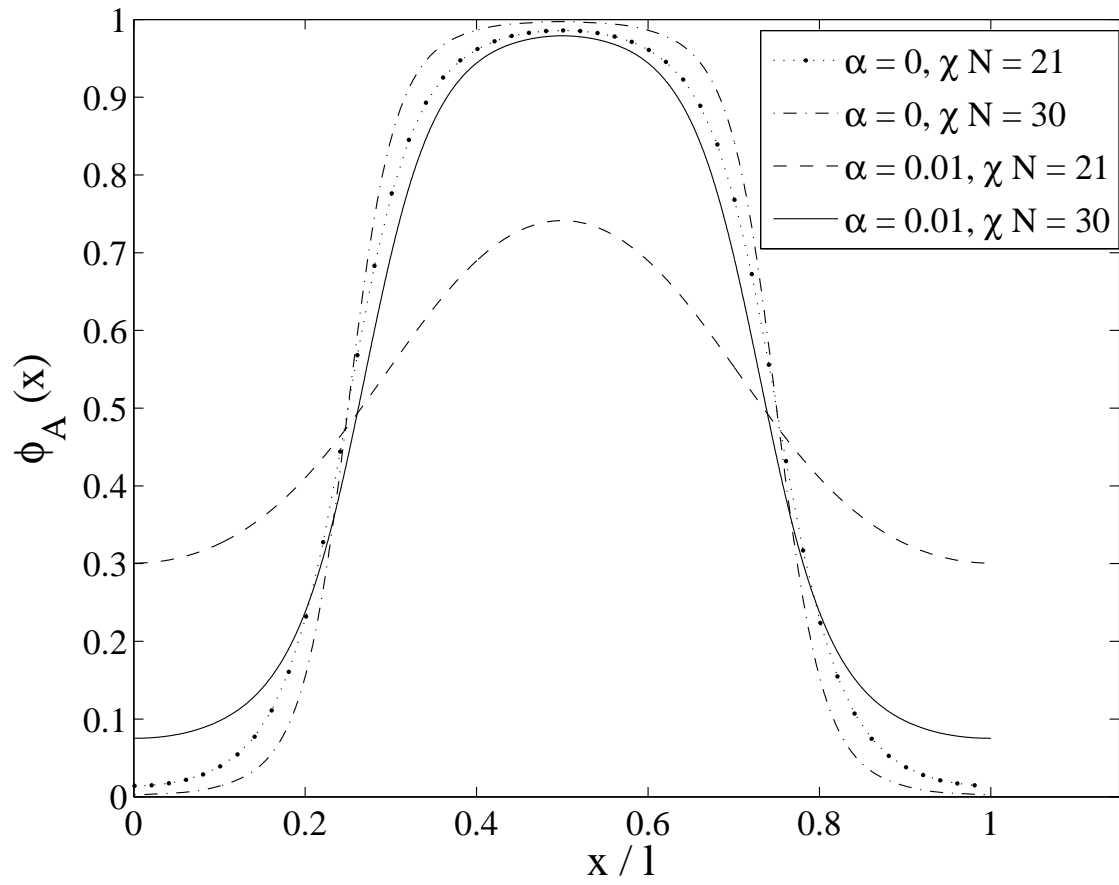


FIG. 8:

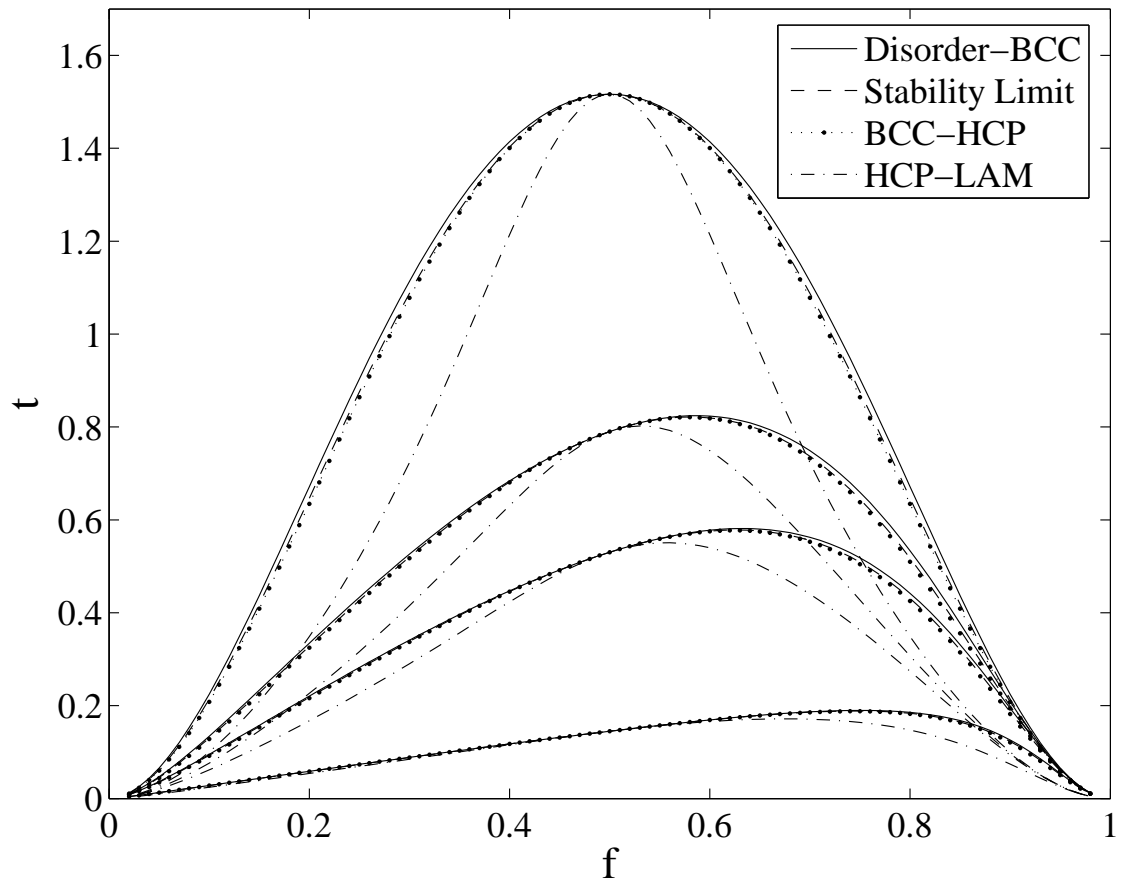


FIG. 9:

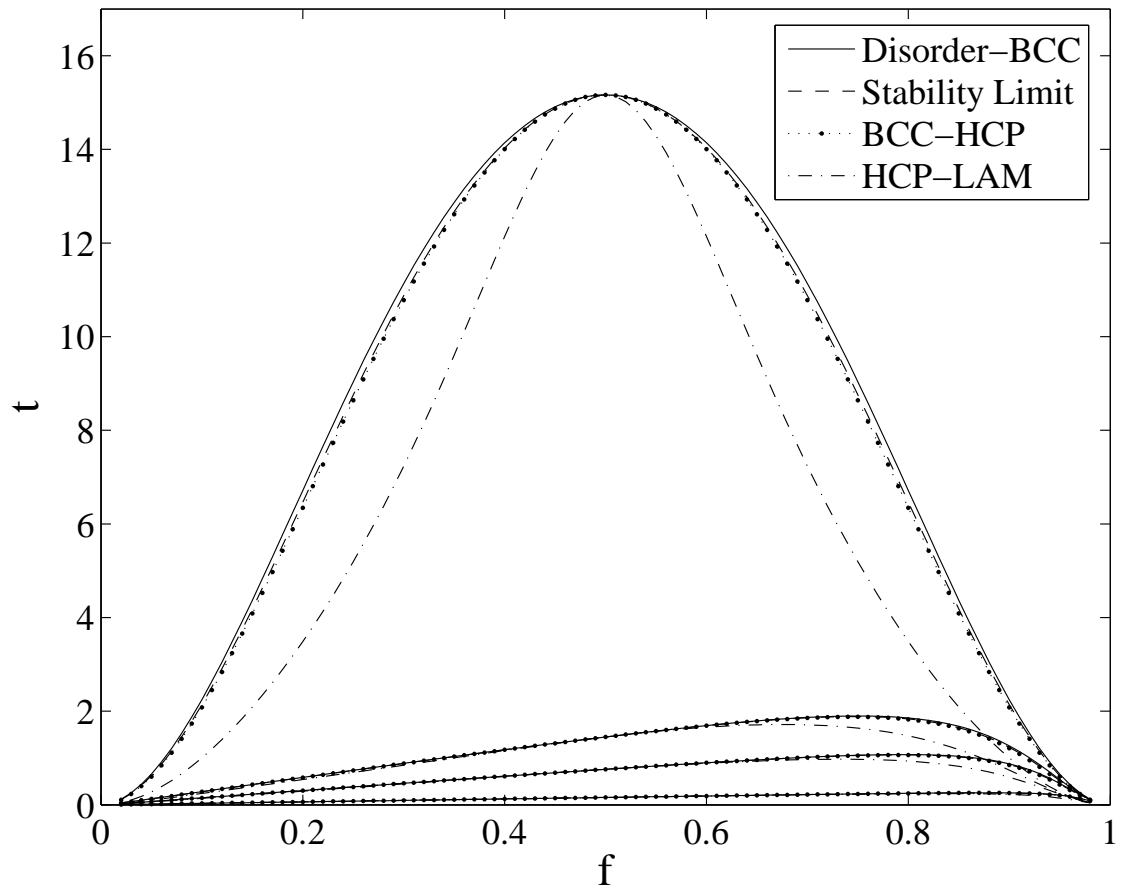


FIG. 10: